

Surface modification of PMMA polymer in the interaction with oxygen-argon RF plasma

M. Jafari¹, D. Dorranian^{2*}

¹Department of Physics, Basic Sciences Faculty, Tehran Central Branch, Islamic Azad University, Tehran, Iran

²Plasma Physics Research Center, Science and Research Branch, Islamic Azad University, Tehran, Iran

Received: 12 May 2011/Accepted: 15 August 2011/ Published: 20 September 2011

Abstract

In this experimental research the effects of oxygen-argon plasma on the structure and morphology of Poly Methyl Methacrylate (PMMA) polymer doped with orange L-3R dye is investigated. Samples with 0.2 mm thickness were produced by drying the solution of PMMA granule in dichloromethane. Experiment was carried out in a low pressure chamber with plane electrodes. Plasma was generated with a RF source of 13.56 MHz frequency at 70 W output power. Samples were exposed to different fraction of oxygen-argon plasma for 5 minutes. Based on AFM results surface roughness of samples is significantly altered and the water contact angle is decreased noticeably. With increasing oxygen in the working gas up to 80% the structure of polymer surface and its surface energy are increased leads to removal of grooves on polymer samples. Change of absorption coefficient and the energy gaps of treated polymers are calculated from their UV-NIR-VIS transmission spectrum.

PACs: 61.25.Hk; 82.33.Xj; 78.40.Me; 47.57.Mg

Keywords: PMMA; Surface structure; Energy gap; AFM, Plasma treatment.

1. Introduction

As a result of extensive research and development, polymers have become the fastest growing segment of materials since world war II, with hundreds of polymers being used in an increasing number of applications [1]. In recent years, an increased trend in replacing traditional materials such as glass, metals, and paper by polymeric materials is noticeable in various industries. Comparability of physical and chemical characteristics of polymers to those of conventional materials and their relatively low cost are the primary reasons for this increased trend [2]. Polymeric materials have unique properties such as low density, light weight, and high flexibility [1, 2]. The applications of polymer include films for food packaging, electrical insulation, resins for photoresists, advanced composites possessing superior mechanical properties, a variety of biopolymers, several kinds of packaging, water tubes, window profiles, and lenses for glasses [3, 4]. Polymers are selected for a given application on the basis of their physical, electrical, and chemical properties, e.g., thermal stability, coefficient of thermal expansion, toughness, dielectric constant, dissipation factor, solvent absorption, and chemical resistance [5]. Most polymeric surfaces as well as PMMA are inert, hydrophobic in nature and usually have a low surface energy. Therefore, they do not possess

specific surface properties needed in various applications, and their surfaces need to be treated to obtain polymers with desired surface properties in various instances [6]. Therefore in many applications there is a need to modify the polymer surface with keeping their desired unchanged bulk properties [20], so surface treatment of polymer materials is a domain of growing interest. Plasma processes are widely used in a variety of applications including deposition [7,8], etching [16–19] and a variety of surface modifications [9]. Especially, surface modifications of polymers with plasma processes are expected to be one of the most promising techniques as low-temperature activation and control methods of polymer surface for advanced engineering applications. In the surface modifications of polymers, interactions of ions and radicals impinging onto the polymer surface play important roles. However the ion bombardment with excessive kinetic energy for breaking chemical bonds of polymers and/or deposited films may cause degradation of the polymer surface and/or undesired creation of defects in the deposited films [10]. For successful modification of polymer surface with plasma processes, it is of great significance to avoid unwanted degradation of chemical bonding structures of weak organic molecules due to exposure with ions, radicals, photons and electrons via polymer degradation processes [11–14]. A plasma treatment is a convenient way to obtain modifications without affecting the overall quality of the material [15]. Plasma technique seems to be powerful because its low temperature could be applied to a large variety of materials and could change the surface properties to a large extent. In this work, a mix-

*Corresponding author: Davoud Dorannian;

E-mail: doran@srbiau.ac.ir

Tel: (+98) 021 44869654

Fax: (+98) 021 44869640

ture of oxygen and argon gasses RF plasma is employed for treatment of orange L-3R dye doped PMMA films.

2. Experimental

2.1. Sample preparation

The orange L-3R dye doped PMMA film was prepared by dissolving PMMA granule and orange L-3R dye in dichloromethane. PMMA granule was provided by Yazd Polymer Talaei (YPT) Co., Tehran, Iran. PMMA and L-3R structures are shown in Figs. 1(a) and (b) respectively. 15gr PMMA with 0.03 gr orange L-3R dye was dissolved in 180 ml dichloromethane. The viscous solvent was poured on a flat glass in a closed box. Solution was dried in closed atmosphere at room temperature for 24 hours to obtain 0.2 mm thick orange L-3R dye doped PMMA film.

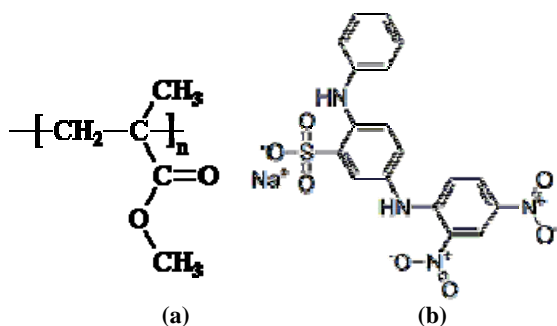


Fig. 1. Chemical structure of PMMA (a) and orange L-3R dye (b).

2.2. Treatment processing

PMMA film was cleaned ultrasonically in distilled water and was exposed to RF oxygen and argon plasma for 5 minutes. Films were located in RF system in such a way that electric field was parallel to their surfaces so energetic particles did not heat the surface of samples normally. Variable of this research was the content of oxygen in working gas. The content of oxygen in working gas for different samples is presented in Table 1. Radio frequency glow discharge plasma was generated at RF frequency of 13.56 MHz and power of 70 W. Base pressure of plasma reactor was 0.001 Torr which was increased to 0.5 Torr after gas feeding.

Table 1. The content of oxygen in working gas for different samples

| Sample | 1 | 2 | 3 | 4 | 5 | 6 |
|----------------|----------|---|-----|-----|-----|-----|
| $O_2/(O_2+Ar)$ | Pristine | 0 | 0.2 | 0.4 | 0.6 | 0.8 |

2.3. Diagnostics

Total Reflectance Fourier transform infrared (ATR – FTIR) analysis was performed using Thermo Nicolet 870 instrument to study the intermolecular interactions between plasma and polymer. The surface morphology of the PMMA samples was studied by AFM using Auto Probe CP atomic force microscope from Park Scientific Instrument. The microstructure of thin films was observed using scanning electron microscope XL30 Models from Philips Company with Holland & Bal – Tec Au coating system. Static water and diiodo – methane drop contact angle measurement was carried out using the sessile drop method on a Kruss G10 contact angle measuring equipment. In the sessile drop experiment, a droplet of a properly purified liquid is put on the solid surface by means of a syringe or a micropipette. The droplet is generally observed by a low magnification microscope, and a resulting contact angle, is measured by a goniometer fitted in the eyepiece. All contact angles are the mean value of four measurements on different parts of the sheets. Polar and disperse parts of the surface tension are obtained by Owens – Wendt and Wu methods. Varian Cary – 500 spectrophotometer was used for recording UV – Vis – NIR transmission and reflection spectrum of the pristine and treated samples.

3. Results and Discussion

3.1. Surface structure

The most important characteristics of the sample surface are determined by the functional groups present in the surface layer. Fourier transform infrared (ATR – FTIR) spectroscopy is used for this purpose. In Fig. 2 the ATR – FTIR spectra of the untreated, samples 2 and samples 6 are shown and the major changes in functional groups of samples is presented in Table 2. For sample 3 which were treated with 20% oxygen in working gas number of O – H and C – O bounds are increased. This is the result of oxygen species in plasma, which leads to increasing these chemical bounds. 80% argon in working gas breaks the bounds on polymer surface and free element make new bounds with oxygen. With decreasing argon for the case of sample 3, number of new bounds are decreased but after that increasing the amount of oxygen in the working gas leads to oxidation of more H and N atoms of polymer surface. Changing the surface energy of samples and their optical properties are the results of modification of films structure in contact with oxygen-argon plasma.

3.2. Surface morphology

Changes of morphology of the surface of samples are investigated by AFM micrographs. They are shown in Fig. 3 and the RMS roughness of the surface versus sample number measured by AFM probe is plotted in

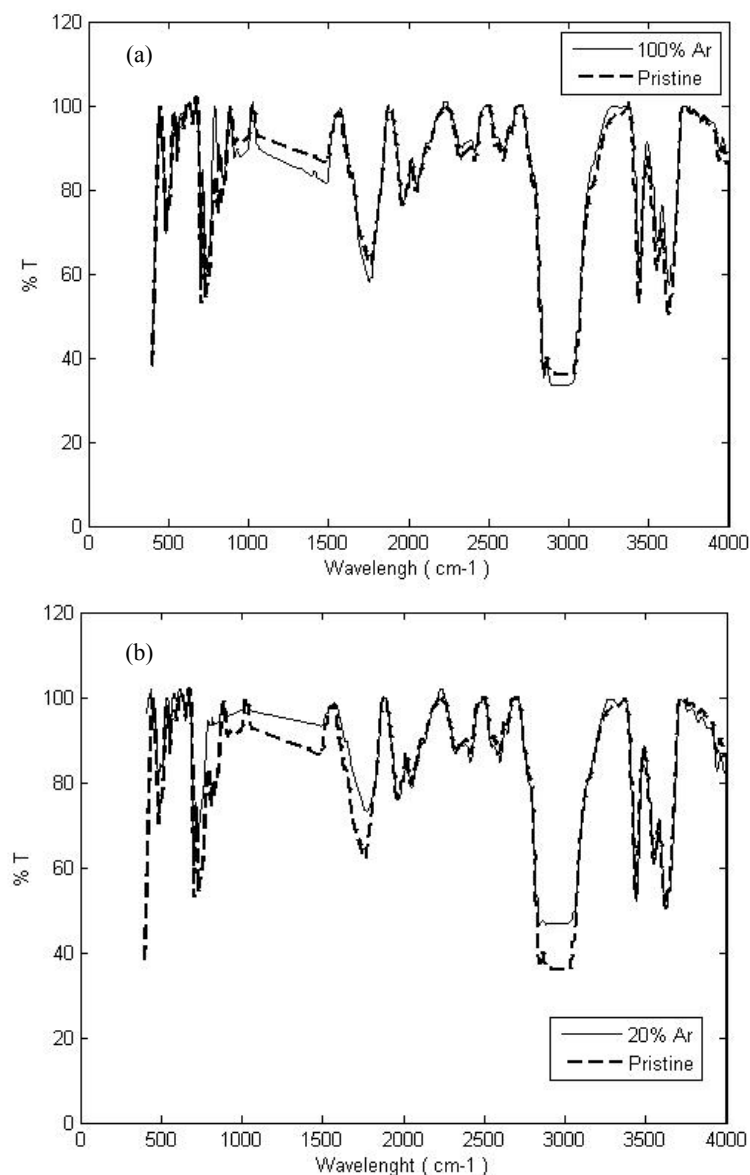


Fig. 2. ATR-FTIR spectrum for pristine sample in comparison with sample 2(a) and sample 6(b).

Fig. 4. RMS roughness are varied from 1.5 to 20 Å. According to the fact that samples were not heated by energetic particles in plasma, the major changes on the surface of samples are due to chemical reactions caused by oxygen and its reactive species in the plasma. The influence of oxygen amount in the morphology of treated surface is clear. The interaction is a kind of etching of surface. One expects that the roughness change has a direct impact on the surface properties,

in particular on the wettability and adhesion property of the samples. As can be seen in Fig. 4 significant effect of oxygen appears when its partial pressure in working gas is more than 0.4.

The microstructure of the thin films was observed using scanning electron microscopy (SEM) which is shown in Fig. 5. Pictures magnification is $\times 15000$ and 1 μm scale is shown on the pictures. Several grooves can be observed on the surface of pristine sample in

Table 2. The magnitudes of the peak intensity of IR transmission of samples.

| Functional group | λ (cm^{-1}) | Sample 1 | Sample 2 | Sample 3 | Sample 4 | Sample 5 | Sample 6 |
|------------------|--------------------------------|----------|----------|----------|----------|----------|----------|
| C-O | 1070 | 89.5 | 92.6 | 97.1 | 90.5 | 92.2 | 96.7 |
| Aromatic | 1500 | 81.6 | 86.3 | 93.4 | 85.2 | 86.8 | 93.3 |
| O-H | 3550 | 61 | 67.7 | 70.6 | 65 | 65.6 | 67 |

Fig. 5 (a). They are due to drying the polymer solution in room temperature. They make polymer unflexible and brittle. After treatment with 60% oxygen in working gas these grooves are disappeared significantly (Fig. 5 (b)) and plasma treatment with 80% oxygen has removed all grooves completely as is shown in Fig. 5 (c). So treatment has increased the flexibility of samples. This is the effect of increasing of surface energy.

3.3. Contact angle and surface energy

The wetting properties of samples are investigated using contact angle measurements. The wetting ability is the ability of a liquid to adhere to a solid and spread over its surface. Hydrophilicity is a characteristic of materials exhibiting an affinity for water. Such materials readily adsorb water. One way for characterizing the surface hydrophilicity is to measure the contact

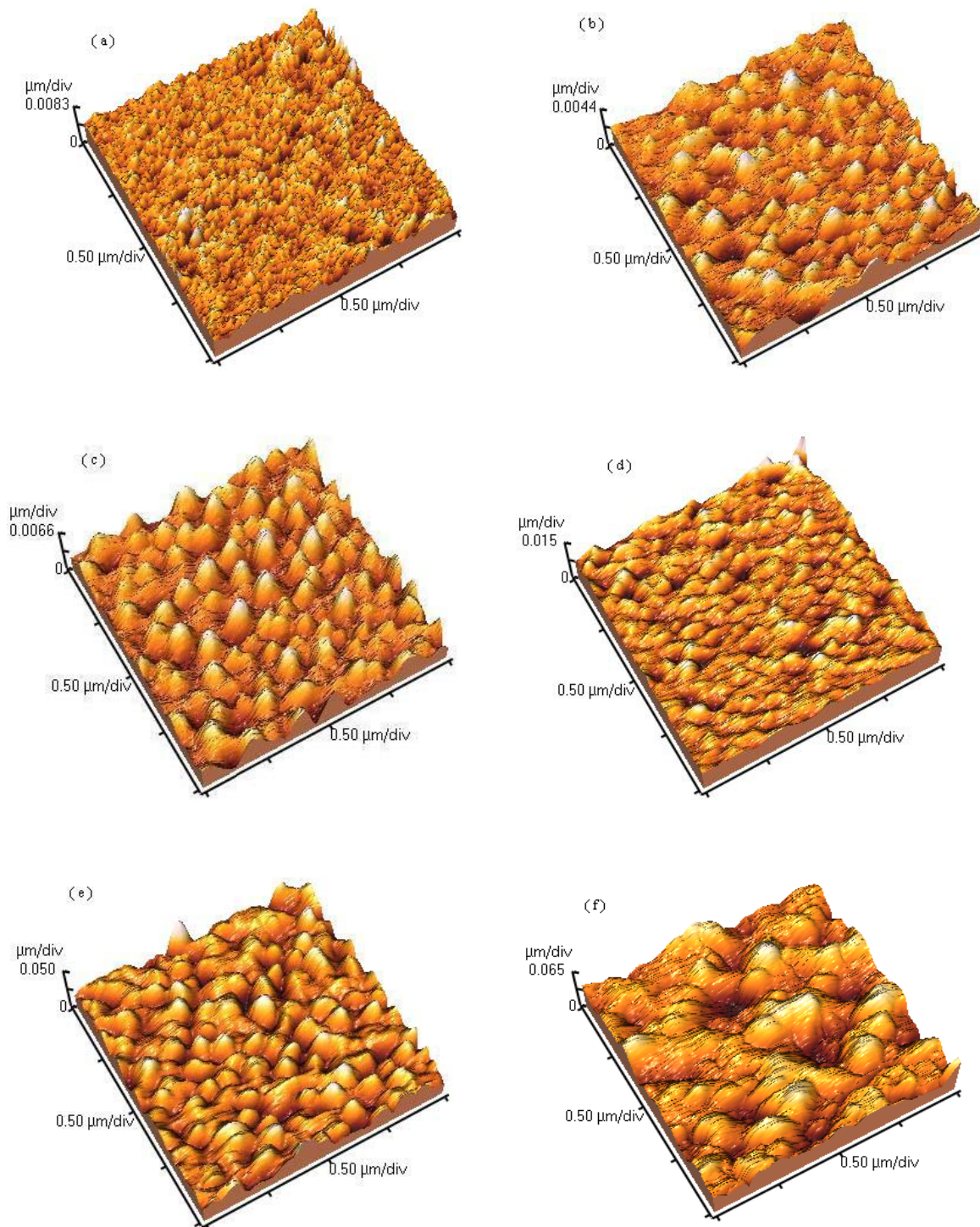


Fig. 3. AFM micrographs of samples 1-6 indicated with a-f, respectively.

Table 3. Values of disperse and polar parts of surface energy, and water and diodo-methan contact angles on the surface of pristine sample and oxygen – argon treated samples.

| Samples number | Water Contact Angle (°) | Diodo Methane Contact Angle (°) | γ_s^p (mN/m) | γ_s^d (mN/m) |
|----------------|---------------------------|-----------------------------------|---------------------|---------------------|
| 1 | 70.7 | 37.9 | 40.65 | 6.84 |
| 2 | 53.9 | 31.7 | 43.53 | 14.34 |
| 3 | 56.3 | 29.2 | 44.56 | 12.67 |
| 4 | 54.5 | 41.4 | 38.88 | 15.82 |
| 5 | 50.8 | 38.9 | 40.15 | 17.42 |
| 6 | 57.4 | 43 | 38.05 | 14.5 |

angle made by a drop of liquid on the surface at the point where the two phases meet. For a given droplet on a solid surface: the contact angle is a measurement of the angle formed between the surface of a solid and the line tangent to the droplet radius from the point of contact with the solid. A contact angle of zero results in wetting, while an angle between 0 and 90° results in spreading of the drop (due to molecular attraction). Angles greater than 90° indicate the liquid tends to ball-up and run off the surface easily. The contact angle of water and diodomethane drops on the surface of samples is presented in Table 3. As can be seen the water contact angle is decreased noticeably. This is because of increasing the O-H molecules on the surface of samples. It means that the polar part of surface energy is increased. Variation of the contact angle of diodomethane is not significant, shows that the disperse part of surface energy of sample is not changed significantly in the treatment.

For calculating the surface energy Young model is employed. Classical model by Young suggests that:

$$\gamma_{SV} = \gamma_{LV} \cos \theta + \gamma_{SL}, \quad (1)$$

where θ is the measured contact angle, γ_{SV} the surface tension of solid in contact with air, γ_{LV} the surface

tension of the liquid in contact with air, and γ_{SL} is the surface tension between the solid and the liquid. The work of adhesion W_a between the solid and liquid can be expressed in terms of the Dupre equation as follows:

$$W_a = \gamma_{SV} + \gamma_{LV} - \gamma_{SL}. \quad (2)$$

By combining these two equations, the Young – Dupre equation becomes:

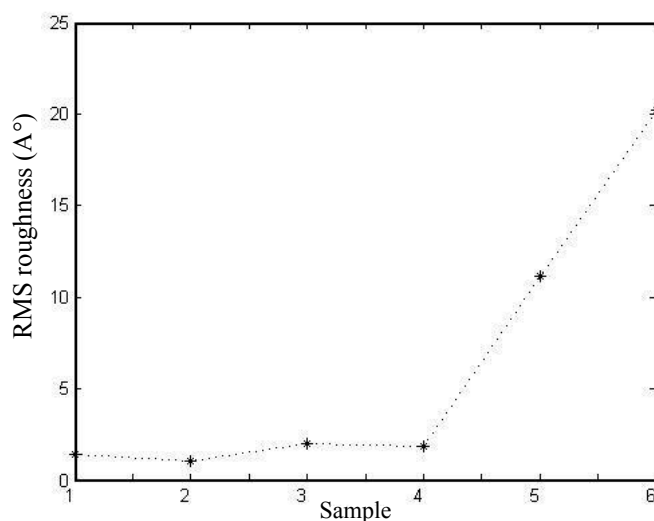
$$W_a = \gamma_{SV}(1 + \cos \theta). \quad (3)$$

The solid surface tension can be separated into the intermolecular attraction of polar interaction γ_s^p and dispersion interaction γ_s^d as:

$$\gamma_s = \gamma_s^d + \gamma_s^p. \quad (4)$$

Therefore, the work of adhesion can be expressed as the sum of the different intermolecular forces at the interface.

$$W_a = 2(\gamma_{LV}^d \gamma_s^d)^{1/2} + 2(\gamma_{LV}^p \gamma_s^p)^{1/2}. \quad (5)$$

**Fig. 4.** RMS roughness of surface versus sample number.

Then

$$\gamma_{LV}(1 + \cos \theta) = 2(\gamma_{LV}^d \gamma_s^d)^{1/2} + 2(\gamma_{LV}^p \gamma_s^p)^{1/2} \quad (6)$$

For water: $\gamma_{LV} = 72.8 \text{ mN/m}$, $\gamma_{LV}^d = 21.8 \text{ mN/m}$, $\gamma_{LV}^p = 51.0 \text{ mN/m}$.

and for diodomethane: $\gamma_{LV} = 50.8 \text{ mN/m}$, $\gamma_{LV}^d = 49.5 \text{ mN/m}$, $\gamma_{LV}^p = 1.3 \text{ mN/m}$ [10,14].

The surface energy depends on the liquid used for measurement, and the polar and disperse (non-polar) components of the surface energy are determined by using polar and non-polar solvents. In order to understand the hydrophilic and hydrophobic modifications achieved on PMMA surface due to RF plasma treatment water and diodomethane, γ_s^p and γ_s^d values of total surface energy and the water and diodomethane contact angle values are tabulated in Table 3. RF plasma with different percentages of oxygen in the working gas, although does not make specific changes in nonpolar surface energy, but increases the polar part of the energy levels which in turn increases the total energy surface of polymer. The surface energy of samples is shown in Fig. 6. Generally it can be claimed a part of our goal which is increasing the surface energy of PMMA is achieved. It can be seen that the water contact angle of polymer surface is decreased and hydrophilicity of polymer is increased by

plasma treatment.

3.4. Absorption coefficient and band gap energy

$T(\lambda)$, the transmittance spectrum of samples in the UV-Vis-NIR region is measured at room temperature. Using this spectrum in the relation:

$$\alpha = \frac{1}{d} \ln \left[\frac{1}{T} \right], \quad (7)$$

α the absorption coefficient of samples is extracted. Variation of absorption coefficient of samples is plotted in Fig 7. Two absorption peaks at 280 nm and 470 nm wavelength can be observed. According to references the peak at 280 nm belongs to PMMA while the peak at 470 nm is related to orange L-3R color. Almost for all samples the absorption coefficient is increased after treatment. This increase is proportional to the amount of oxygen in the working gas.

The optical band gap is the value of optical energy gap between the valance band and the conduction band. The optical band gap of the samples is determined from the absorption spectra near the absorption edges. The photon absorption in many amorphous materials is found to obey the Tauc relation [4, 20], which is of the form:

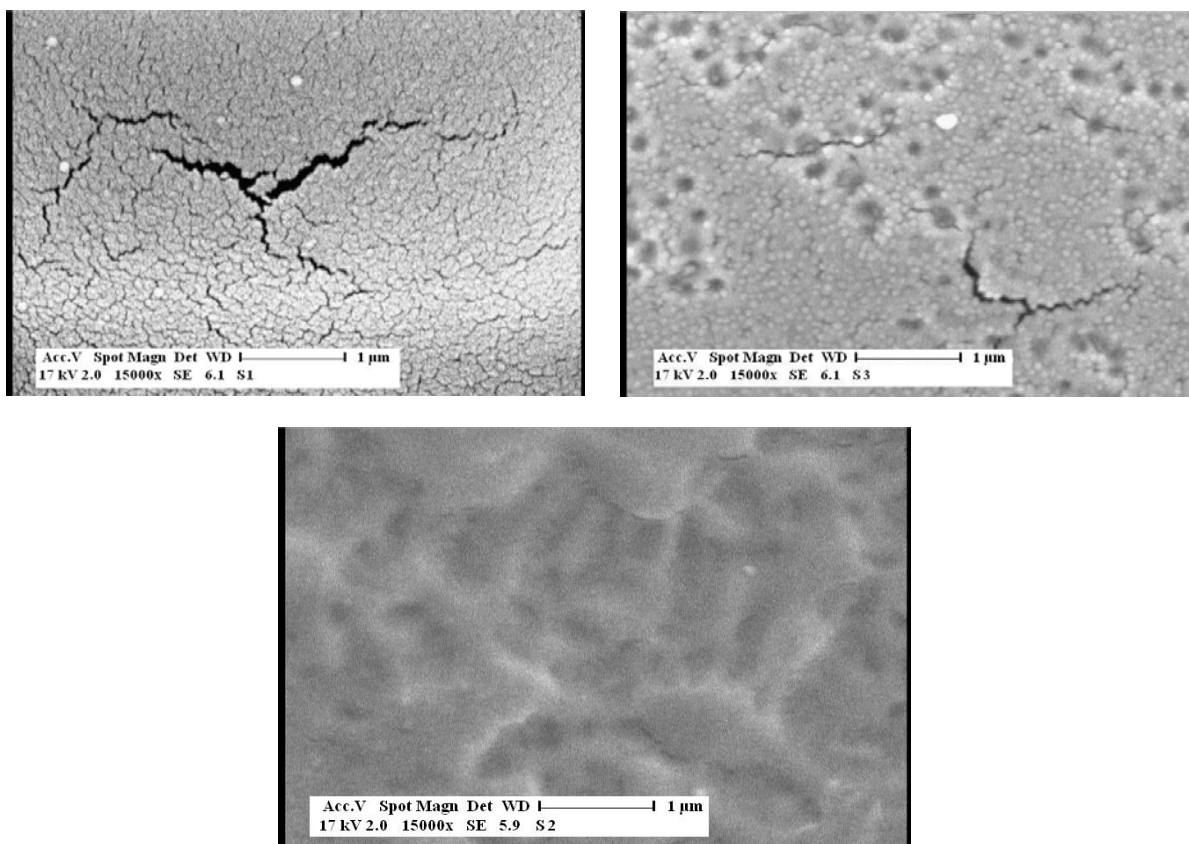


Fig. 5. SEM microstructure of PMMA matrix composite in sample 1 (a), sample 5 (b) and sample 6 (c).

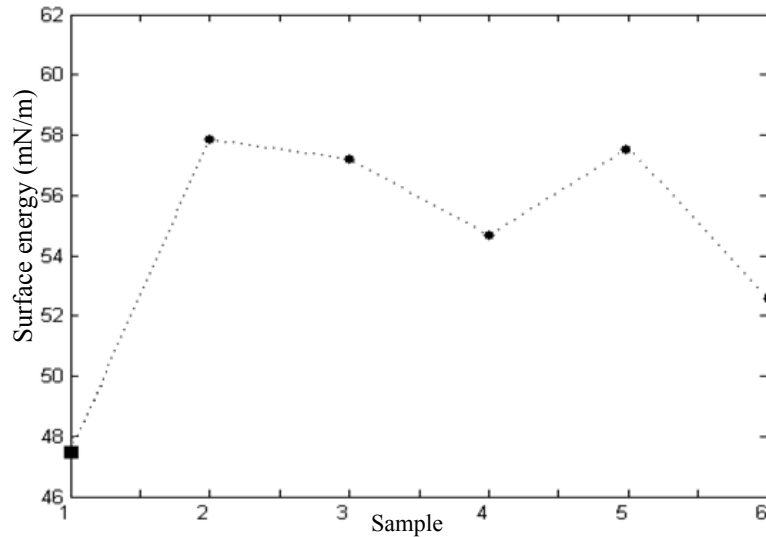


Fig. 6. Surface energy of treated samples versus samples number.

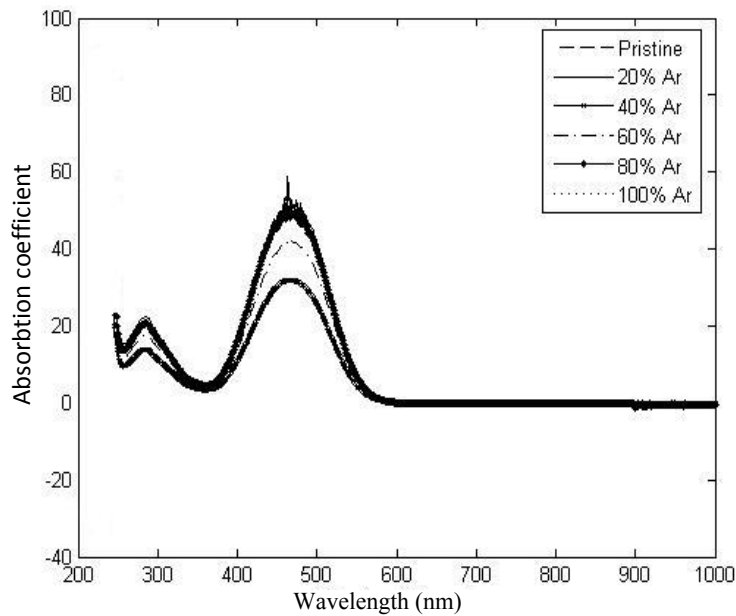


Fig. 7. Absorption coefficient and sample chart of crude plasmas samples under 70 watts.

$$\alpha h\nu = \beta(h\nu - E_g)^n \tag{8}$$

where E_g is the band gap energy, α is the absorption coefficient, $h\nu$ is the photon energy, factor β depends on the transition probability and can be assumed to be constant within the optical frequency range [21], and the n is related to the distribution of the density of states. The index n has discrete values like 1/2, 3/2, 2 or more depending on whether the transition is direct or indirect and allowed or forbidden, respectively. In the direct and allowed cases, the index $n = 1/2$ whereas for the direct but forbidden cases it is 3/2. But for the indirect and allowed cases $n = 2$ and for the forbidden cases it is 3 or more. The value of n for samples is estimated from the slope of the $\log(\alpha)$ vs. $\log(h\nu)$ plots by taking a linear fit is found to be 2 [21,

22]. To calculate E_g , the usual method is plotting $(\alpha h\nu)^{1/n}$ against $h\nu$. The values of the band gap energy of pristine and treated samples are tabulated in

Table 4. E_g values for different samples in eV

| Samples | E_g | E_g |
|----------|-------|-------|
| Pristine | 3 | 4.79 |
| 100% Ar | 3.06 | 4.76 |
| 80% Ar | 2.96 | 4.72 |
| 60% Ar | 3.03 | 4.79 |
| 40% Ar | 3.03 | 4.82 |
| 20% Ar | 2.96 | 4.75 |

Table 4. As can be seen this magnitude is not changed significantly in the treatment process due to low power of the applied plasma.

4. Conclusion

In this experiment, the results of PMMA polymer surface exposed to RF plasma with mixture of oxygen and argon as the working gas is investigated. Results prove that argon atoms break the bonds of sample surfaces and oxygen species change the structure chemically. AFM images show that surface is etched by active oxygen species. Energy of the polymer surface is increased in this experiment which is confirmed by decreasing the grooves on the surface of polymer as can be seen in the SEM images. Treatment has also changed the main optical parameter of samples such as transmission and absorption coefficient. But band gap of samples is not changed significantly by the treatment.

References

- [1] N. L. Singh, A. Qureshi, F. Singh, D. K. Avasthi, *Mater. Sci. Eng. B* **137**, 85 (2007).
- [2] Y. Fu, Ricky, I. T. L. Cheung, Y. F. Mei, C. H. Shek, G. G. Siu, K. Chu Paul, W. M. Yang, Y. X. Huang, X. B. Tian, S. Q. Yang; *Nucl. Ins. Meth. Phys. Res. B* **237**, 417 (2005).
- [3] H. Kaczmarek, H. Chaberska; *Appl. Sur. Sci.* **252**, 8185 (2006).
- [4] F. Yakuphanoglu, G. Barim, I. Erol, *Physica B* **391**, 136 (2007).
- [5] W. S. Kim, Y. C. Jeong, J. K. Park, C. W. Shin, N. Kim, *Opt. Mater.* **29**, 1736 (2007).
- [6] M. Ozdemir, C. U. Yurteri, H. Sadikoglu, *Critical Rev. Food Sci. Nutrition* **39**, 457 (1999).
- [7] A. Palmero, N. Tomozeiu, A. M. Vredenberg, W. M. Arnold-bik, F. H. P. M. Habraken, *Surf. Coat. Tech.* **215**, 177 (2004).
- [8] R. Snyders, J-P. Dauchot, M. Hecq, *Plasma Process. Polym.* **4**, 113 (2007).
- [9] E. T. Kang, Y. Zhang, *Adv. Mater.* **12**, 1481 (2000).
- [10] C-M. Chan, T-M. Ko, H. Hiraoka, *Surf. Sci. Rep.* **24**, 1 (1996).
- [11] T. Steckenreiter, E. Balanzat, H. Fuess, C. Trautmann, *Nucl. Instrum. Meth. Phys. Res. B* **131**, 159 (1997).
- [12] M. Day, D. M. Willes, *Appl. J. Polym. Sci.* **16**, 203 (1972).
- [13] S. Maseya, P. Cloutierb, L. Sancheb, D. Roy, *Rad Phys. Chem.* **77**, 889 (2008).
- [14] S. I. Stolarova, P. R. Westmorelanda, M. R. Nydenb, G. P. Forney, *Polymer* **44**, 883 (2003).
- [15] K. Kutasi, N. Bibinov, A. Von Keudell, K. Wiesemann, *Optoelect. Ad. Mater.* **7**, 2549 (2005).
- [16] C. J. Mogab, A. C. Adams, D. L. Flamm, *Appl. Phys. J.* **49**, 3796 (1978).
- [17] J. W. Butterbaugh, D. C. Gray, H. H. Sawin, *Vac. Sci. Technol. J. B* **9**, 1461 (1989).
- [18] T. Ono, T. Mizutani, Y. Goto, T. Kure, *Jpn Appl. Phys. J* **39**, 5003 (2000).
- [19] M. Nagai, T. Hayashi, M. Hori, H. Okamoto, *Jpn. Appl. Phys. J.* **45**, 7100 (2006).
- [20] S. Saravanan, M. R. Anantharaman, S. Venkatachalam, D. K. Avasthi; *Vacuum* (2007).
- [21] H. M. Zidan, M. Abu-Elander, *Physica. B* **355**, 308 (2005).
- [22] U. S. Sajeev, C. J. Mathai, S. Saravanan, R. R. Ashokan, S. Venkatachalam, M. R. Anantharaman, *Bull. Mater. Sci.* **29**, 159 (2006).
- [23] D. Dragoman, M. Dragoman, *Optical characterization of solids*, 1stedn, Springer, Berlin (2002).